Molecular Modeling of Phenothiazines and Related Drugs As Multidrug Resistance Modifiers: A Comparative Molecular Field Analysis Study

Ilza Pajeva[†] and Michael Wiese*[,‡]

Center of Biomedical Engineering, Bulgarian Academy of Sciences, BG-1113 Sofia, Bulgaria, and Department of Pharmacy, University of Halle, D-06120 Halle, Germany

Received November 18, 1997

A set of 40 phenothiazines, thioxanthenes, and structurally related drugs with multidrug resistance modulating activity in tumor cells in vitro were selected from literature data and subjected to three-dimensional quantitative structure−activity relationship study using comparative molecular field analysis (CoMFA). More than 350 CoMFA models were derived and evaluated using steric, electrostatic, and hydrophobic fields alone and in combination. Four alignment strategies based on selected atom pairs or field fit alignment were compared. Several training and test sets were analyzed for both neutral and protonated drug forms separately. Each chemical class was trained and tested individually, and finally the classes were combined together into integrated models. All models obtained were statistically significant and most of them highly predictive. All fields contributed to MDR reversing activity, and hydrophobic fields improved the correlative and predictive power of the models in all cases. The results point to the role of hydrophobicity as a space-directed molecular property to explain differences in anti-MDR activity of the drugs studied.

Introduction

Multidrug resistance (MDR) is a major obstacle to successful treatment of metastatic cancers. It is a broad-spectrum resistance to chemotherapy and several mechanisms are proven to be involved in its acting.[1] "Typical" or "classical" MDR is associated with the product of *MDR1* gene, the membrane integrated transport protein P-glycoprotein (P-gp). P-gp is thought to recognize a large variety of cytotoxic agents as substrates for ATP-dependent efflux, thereby reducing their intracellular accumulation.[2] Simultaneously, a number of drugs have been identified that are not cytotoxic by themselves (calcium channel blockers, anti-arrhythmics, antidepressants, antipsychotics and many others) but can reverse P-gp-related MDR.[3−5] These drugs, called MDR reversing agents (modulators, chemosensitizers, reverters), represent a wide range of chemical structures and can exert different cellular effects; however, they are supposed to act by the same mechanism for the reversal of MDR. The most widespread concept presumes inhibition of P-gp activity by competition with the cytotoxic agents for the same binding sites.[6] Although there is still considerable controversy about the mechanism of action of the efflux pump, it is well recognized that the MDR modulators share common physicochemical features needed for the reversal: they are amphipathic drugs and mostly protonated.[2] Our previous investigations on membrane activity of some catamphiphilic MDR reverters (phenothiazines, thioxanthenes, and structurally related drugs) suggest that these common features relate directly to the ability of the chemosensitizers to interact with the membrane phospholipids.[7] Recent studies on photoaffinity label sites and point mutations of P-gp revealed that the parts of the protein that affect its transport specificity belong mainly to amino acid sequences located in the membrane.[2] It was also shown that potent MDR modulators inhibit the membrane binding of rhodamine-G6 even in the absence of any P-gp or other proteins.[8] These findings point to mechanisms of MDR reversal mediated by drug−membrane interactions.

Conformational and molecular modeling studies of phenothiazines, thioxanthenes, and similar drugs reported so far are mostly related to their anti-calmoduline,[9] anti-dopamine,[10−13] and antitumor activity.[14] Whereas a good correlation between anti-calmoduline and antiproliferative activity has been reported, no correlation between anti-calmoduline and MDR modulating activity has been observed for these drugs.[15] Pearce and co-workers compared the conformations of some reserpine and yohimbine analogues to that of the powerful MDR modulator verapamil, as well as of chlorpromazine and chloroquine, and concluded that the relative disposition of aromatic rings and basic nitrogen was important for their anti-MDR activity in vinblastine resistant human leukemia cells.[16] They postulated the existence of a conserved structural element for binding to the putative MDR receptor associating it with P-gp.

Recently, we performed a QSAR study of a number of phenothiazines, thioxanthenes, and structurally related drugs that are known to reverse MDR in vitro in different resistant tumor cell lines.[15,17−19] We identified and quantitatively estimated several structural features of significant importance for their anti-MDR activity.[20] To decide on possible space property differences related to anti-MDR activity, we performed as well a conformational and molecular modeling study of two powerful reverters—*trans*- and *cis*-flupentixol.[20,21] We suggested

* The author to whom inquiries should be addressed; phone +49 345 552 50 40, fax +49 552 70 18, e-mail wiese@pharmazie.uni-halle.de.

[†] Center of Biomedical Engineering, Bulgarian Academy of Sciences; e-mail pajeva@iph.bio.acad.bg.

[‡] Department of Pharmacy, University of Halle.

S0022-2623(97)00786-3 CCC: $15.00
Published on Web 05/05/1998

that the 2−3-fold difference in their MDR reversing activity might be due to differences in their lipophilic and electrostatic fields causing different orientations of the molecules in the membrane lipid environment. Thus, despite the common physicochemical "rules" proposed, it is likely that modulators of P-gp MDR also possess some specific structural determinants that remain to be established.

In this paper we report a 3D QSAR study of 40 MDR modulators from classes of phenothiazines, thioxanthenes, and structurally related drugs by the CoMFA approach. It is based on our previous results on membrane interactions, QSAR and molecular modeling studies of some of these compounds.[7,20,21] Considering hydrophobic interactions to represent an essential part of the drug−membrane interaction, hydrophobic fields were also included as possible descriptors of molecular recognition capabilities[22] in addition to the standard CoMFA Lennard-Jones and Coulomb-type potentials. As shown in the study, hydrophobicity contributes significantly to the CoMFA correlative, predictive, and interpretative power in most cases. The main goal of the study was to obtain 3D QSAR models of good statistical predictivity and possibly more information about the drugs' specific properties associated with MDR reversal. To the best of our knowledge this is the first attempt to derive 3D QSAR models of MDR reverters using CoMFA.

Results and Discussion

Cytotoxicity and MDR Reversing Activity. Table 1 lists the names, structures, and observed MDR reversing activity values (MDR ratios) of the drugs used in the study.

A plot of MDR ratio versus IC_{50} for cell growth inhibition of the drugs is presented in Figure 1. In the figure, logarithmic values for both MDR ratio and IC_{50} were used, and the inverse of IC_{50} was taken to obtain higher cytotoxicity values for the more active MDR modifiers. The plot confirms the reported observation of Ford et al.[15] on some of these drugs about the lack of correlation between drugs' own cytotoxic and MDR reversing activities. As can be seen from the figure, no dependence between chemosensitizing activity and the direct antiproliferative effect for all 40 drugs can be outlined. This points out different mechanisms of cytotoxicity and MDR reversal of the compounds under investigation.

CoMFA-Related Parameters. In CoMFA there are a number of prerequisites and parameters that can be set by the user so as to influence the final results.

The alignment of the molecules is one of the most important criteria determining the quality of the 3D-QSAR models and can greatly affect the outcome of the analysis. In this study two types of alignment were used and compared, provisionally called *skeleton* and *shape*. The skeleton alignment is based on the skeleton of the tricyclic ring system and is achieved by fitting the corresponding non-hydrogen atoms of the three rings. Shape alignment is based on the previously proposed pharmacophoric scheme derived from the QSAR free-Wilson analysis and molecular modeling.[20,21] It is achieved by fitting the centroids of the two aromatic moieties in the tricyclic ring system and the first basic nitrogen in the aliphatic chain (Figure 2). According to this alignment the ring systems of the target and template molecules can be oriented equally (Figure 2a) or mirror-like (Figure 2b) in relation to the substituent on the second position of the ring system to yield the lowest rms values. Additionally, the CoMFA field fit alignment technique was applied to each alignment separately, leading to a total of four alignments for both the neutral and protonated drugs.

To avoid chance correlations, several training and test data sets were created and evaluated (Table 1): (1) training on 17 phenothiazines (numbers 1−17) and test on 9 drugs (numbers 18−21, 36−40); (2) training on 21 phenothiazines (numbers1−21) and test on 16 thioxanthenes and related drugs (numbers 22−40); (3) training on 16 thioxanthenes (numbers 22−36) and test on 21 phenothiazines and related drugs (numbers 1−21, 38−40); (4) training on 37 phenothiazines and thioxanthenes (numbers 1−37); (5) training on all 40 compounds.

To decide on the most relevant CoMFA parameters to be set in the study, preliminary investigations on the influence of the CoMFA field type and threshold column filtering (σ_{min} or field variance at each grid point) on the statistical parameters of the models were undertaken using the skeleton aligned training set of 17 phenotiazines (numbers 1−17, Table 1). The corresponding results are presented in Table 2. At 30 kcal/mol energy field cutoff and $\sigma_{min} = 0$, the best $Q^2_{cv} = 0.879$ was obtained for the CoMFA B field. It should be stated that this field combines both the steric and electrostatic interaction energies; however, as can be seen from Table 2, Q^2_{cv} and the contributions of the steric and electrostatic fields differ from that of the combination of S & E fields taken separately. [This is due to the fact that, in the SYBYL CoMFA implementation, in case of the B field, the electrostatic field is assigned a missing value inside atoms and is therefore fully ignored at those points while, in case of the electrostatic field calculated separately, it is set to the selected cutoff value (positive or negative) inside atoms and subsequently taken into account in the PLS analysis. The other CoMFA fields also showed high Q^2_{cv}. A decrease in Q^2_{cv} by 0.11 was observed when B fields were used, increasing σ_{min} from 0 to 2 kcal/mol (Table 2). Although it is thought that the signal-to-noise ratio improves at higher σ_{min}, Q^2_{cv} decreased by more than 10%, setting σ_{min} to 2 kcal/mol. At $\sigma_{min} = 0.2$ kcal/mol, the computational time was about 2 times lower in comparison to $\sigma_{min} = 0$ while the decrease in Q^2_{cv} was negligible. Thus, $\sigma_{min} = 0.2$ kcal/mol was set in all further calculations as the threshold column filtering value.

As each field individually yielded an acceptable model, in all further calculations the different fields were systematically explored alone and in combination in order to identify those of them that yield the best models. The comparison of different models was used for lateral validation.

CoMFA Models of Phenothiazines. The first CoMFA models were derived using the training set of 17 skeleton aligned phenotiazines (Table 1, numbers 1−17). This data set was used as a probe training set because of several reasons as explained below. The structural features that are generally considered as

Table 1. Structures and MDR Reversing Activities of Phenothiazines, Thioxanthenes and Structurally Related Drugs Investigated in This Study

Phenothiazines 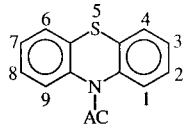

Thioxanthenes 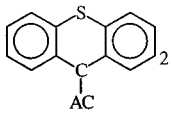

Imipramines 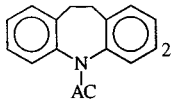

Acridines 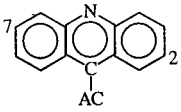

No.	Compound name	Ring system: substiuent	Ring system: position	Aliphatic chain: AC	MDR ratio (±SD)	log (MDR)
	Phenothiazines					
1.	Promazine			$-(CH_2)_3-N(CH_3)_2$	1.2 (±0.2)	0.079
2.	1-Chloropromazine	-Cl	1	" "	1.3 (±0.2)	0.114
3.	Chlorpromazine	-Cl	2	" "	1.6 (±0.3)	0.204
4.	3-Chlorpromazine	-Cl	3	" "	1.3 (±0.2)	0.114
5.	4-Chlorpromazine	-Cl	4	" "	1.4 (±0.3)	0.146
6.	7-Hydroxychlorpromazine	-Cl, -OH	2, 7	" "	1.0 (±0.3)	0.000
7.	3,8- Dihydroxychlorprom.	-Cl, -OH, -OH	2, 3, 8	" "	0.9 (±0.3)	-0.046
8.	7,8- Dihydroxychlorprom.	-Cl, -OH, -OH	2, 7, 8	" "	0.8 (±0.2)	-0.097
9.	Thiomethylpromazine	$-SCH_3$	2	" "	1.5 (±0.2)	0.176
10.	Trifluopromazine	$-CF_3$	2	" "	2.0 (±0.3)	0.301
11.	Didesmethylchlorpromazine	-Cl	2	$-(CH_2)_3-NH_2$	1.1 (±0.1)	0.041
12.	Desmethylchlorpromazine	-Cl	2	$-(CH_2)_3-NH-CH_3$	1.2 (±0.2)	0.079
13.	Chlorproethazine	-Cl	2	$-(CH_2)_3-N(C_2H_5)_2$	2.2 (±0.4)	0.342
14.	Prochlorperazine	-Cl	2	$-(CH_2)_3-N$ 	2.6 (±0.4)	0.415
15.	Trifluoperazine	$-CF_3$	2	" "	3.4 (±0.4)	0.531
16.	Perphenazine	-Cl	2	$-(CH_2)_3-N$ 	2.0 (±0.3)	0.301
17.	Fluphenazine	$-CF_3$	2	" "	2.7 (±0.3)	0.431
18.	2-Chloro-10-[2-(dimethyl-amino)ethyl]phenothiazine	-Cl	2	$-(CH_2)_2-N(CH_3)_2$	1.5 (±0.3)	0.176
19.	2-Chloro-10-[2-(dimethyl-amino)butyl]phenothiazine	-Cl	2	$-(CH_2)_4-N(CH_3)_2$	2.0 (±0.3)	0.301
20.	Promethazine			$-CH_2-CH(CH_3)-N(CH_3)_2$	1.9 (±0.5)	0.279
21.	Chlorpromazine sulfoxide	-Cl, =O	2, 5	$-(CH_2)_3-N(CH_3)_2$	2.2 (±0.4)	0.342
	Thioxanthenes					
22.	trans-7006	-Cl	2	$=CH-CH_2-N$ 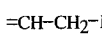	1.6 (±0.4)	0.204
23.	cis-753	-Cl	2	$=CH-(CH_2)_2-N$ 	6.7 (±1.8)	0.826
24.	trans-753	-Cl	2	" "	15.0 (±2.5)	1.176
25.	cis-762	-Cl	2	$=CH-CH_2-N(CH_3)_2$	1.1 (±0.2)	0.041
26.	trans-762	-Cl	2	" "	1.3 (±0.1)	0.114
27.	cis-768	-Cl	2	$=CH-(CH_2)_2-N(C_2H_5)_2$	4.0 (±0.3)	0.602
28.	trans-768	-Cl	2	" "	7.2 (±0.6)	0.857
29.	789	-Cl	2	$-(CH_2)_3-N$ 	9.7 (±2.7)	0.987
30.	cis-796	$-CF_3$	2	$=CH-(CH_2)_2-N(CH_3)_2$	1.8 (±0.2)	0.255
31.	trans-796	$-CF_3$	2	" "	2.8 (±0.3)	0.447
32.	cis-chlorprothixene	-Cl	2	" "	2.0 (±0.6)	0.301
33.	trans-chlorprothixene	-Cl	2	" "	7.0 (±0.9)	0.845
34.	cis-clopenthixol	-Cl	2	$=CH-(CH_2)_2-N$ 	2.6 (±0.4)	0.415
35.	trans-clopenthixol	-Cl	2	" "	15.0 (±2.3)	1.176
36.	cis-flupenthixol	$-CF_3$	2	" "	4.8 (±0.6)	0.681
37.	trans-flupenthixol	$-CF_3$	2	" "	15.2 (±1.9)	1.182
	Related drugs					
38.	imipramine			$-(CH_2)_3-N(CH_3)_2$	2.5 (±0.9)	0.398
39.	2-chloroimipramne	-Cl	2	" "	2.0 (±0.6)	0.301
40.	quinacrine	$-OCH_3$, -Cl	2, 7	$-NH-CH(CH_3)-(CH_2)_3-N(C_2H_5)_2$	1.3 (±0.1)	0.113

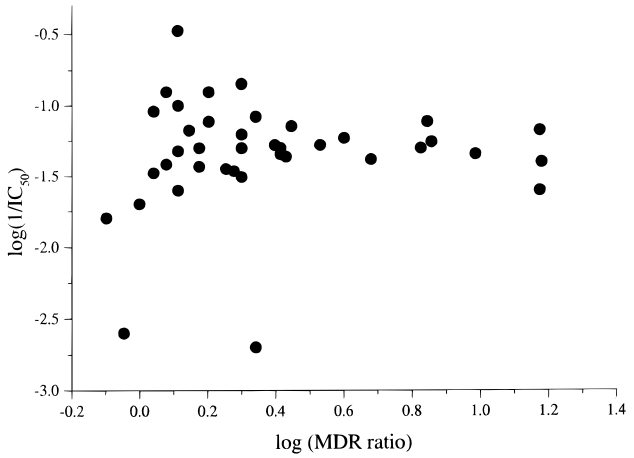

Figure 1. Chemosensitizing (MDR ratio) versus antiproliferative effect (IC_{50} for inhibition of cell growth) of the modifiers studied in 200-fold doxorubicin resistant MCF-7/DOX cells.[15,17]

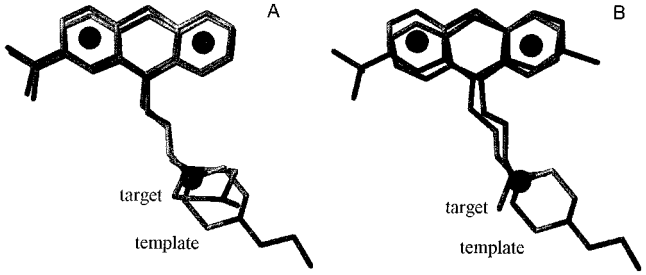

Figure 2. Shape alignment by the centroids of the two aromatic rings and the first basic nitrogen in the aliphatic chain (balls); template molecule, *trans*-flupentixol; alignment technique, rms fitting: A, similar oriented ring systems, target molecule trifluoperazine; B, mirror-like oriented ring systems, target molecule chlorpromazine.

Table 2. Influence of the Standard CoMFA Energetic Fields and Threshold Column Filtering, σ_{min}, on the Statistical Parameters of the CoMFA Models on Phenothiazines (Numbers 1−17, Table 1)

CoMFA field	field cutoff, kcal/mol	σ_{min}, kcal/mol	Q^2_{cv}	N_{opt}	contribution S/E, %
E	30	0.0	0.750	6	0/100
S	30	0.0	0.853	6	100/0
S & E	30	0.0	0.868	6	49/51
B	30	0.0	0.879	6	64/36
B	30	0.05	0.876	7	66/34
B	30	0.10	0.875	7	67/33
B	30	0.20	0.874	7	67/33
B	30	0.30	0.873	7	72/28
B	30	0.50	0.874	7	67/33
B	30	0.75	0.863	6	65/35
B	30	1.00	0.853	5	58/42
B	30	1.50	0.863	6	65/35
B	30	2.00	0.769	7	57/43

physicochemical features shared by P-gp-related MDR modulators are "aromatic ring systems, secondary or tertiary nitrogen atom disposed within an extended side chain and hydrophobicity".[23] Our QSAR study on phenothiazines, thioxanthenes, and related drugs[20] substantiated several structural features of significant importance for anti-MDR activity: the tricyclic ring system and the substituent in position 2, the length of the spacer between the ring system and the first basic nitrogen in the aliphatic chain, the type of the basic nitrogen, and stereoisomery. The training set under investigation is characterized by small structural variation as only the substituents on the tricyclic ring system and the nitrogen vary while the type of ring system and length of the spacer (three methylene groups) remain constant. This allows the estimation of the influence of the substituents on the tricyclic ring system and the substitution pattern of the nitrogen.

Table 3. Comparison of CoMFA Models on Phenothiazines (Numbers 1−17, Table 1)

				field contribution, %		
model	Q^2_{cv}	N_{opt}	SEP_{cv}	S	E	H
E	0.750	6	0.113		100	
S	0.853	6	0.086	100		
S E	0.870	6	0.081	55	45	
B	0.874	7	0.084	67	33	
H	0.664	13	0.238			100
S H	0.929	9	0.072	60		40
E H	0.823	6	0.095	60		40
B H	0.912	7	0.070	50	19	31
B Q^2-GRS	0.883	6	0.077	62	38	

The results are summarized in Table 3. The models with the highest Q^2_{cv} were obtained by combining H and CoMFA steric (SH model) and both fields (BH model). Furthermore, the models B, SH, and BH were recalculated at numbers of components lower than N_{opt}, and the change in SEP_{cv}, was followed. The decrease in the number of components lead to a slight decrease in Q^2_{cv} and up to 14% decrease in SEP_{cv}. The respective non-cross-validated models were then derived and the test set prediction done with them.

Nine compounds of very different structure compared to the training set were used to test the models obtained: three phenothiazines with modified length of the spacer (numbers 18−20, Table 1), one sulfoxide phenothiazine (number 21), two highly potent thioxanthenes (numbers 36 and 37), and three structurally related drugs (numbers 38−40). Their difference in MDR fold reversal was about 10-fold, being 1.182 in log units for the most active *trans*-flupentixol (number37) and 0.182 for the least active 2-chloro-10-[2-(dimethylamino)ethyl]phenothiazine (number 18), thus exceeding significantly the activity range of the training set (−0.097 to 0.531).

The above test set can be considered as a very hard one as the presence of the structural fragments not encountered in the training set and the large difference in the activity range of the training and test set compounds can lead to wrong predictions by any CoMFA model. According to Q^2_{pr}, neither of the models tested could be considered as really successful; however, all Q^2_{pr} were positive (about 0.3), and a relatively good fit (R^2 about 0.6−0.8) of actual versus predicted activities of the tested molecules was observed. (See Table 6 of Supporting Information.) Interestingly, the highest test Q^2_{pr} and R^2 were obtained for the BH model (0.350 and 0.793, respectively), although the SH one showed the highest Q^2_{cv}. In Figure 3 a plot of the predicted versus actual MDR ratios of the test compounds derived from the BH model is presented. As seen from the figure the activities of all test compounds with the exception of quinacrine are underpredicted. Figure 4 shows the residuals of the MDR ratios depending on the data outside the range of the training CoMFA fields for the compounds tested. All tested drugs were novel to some

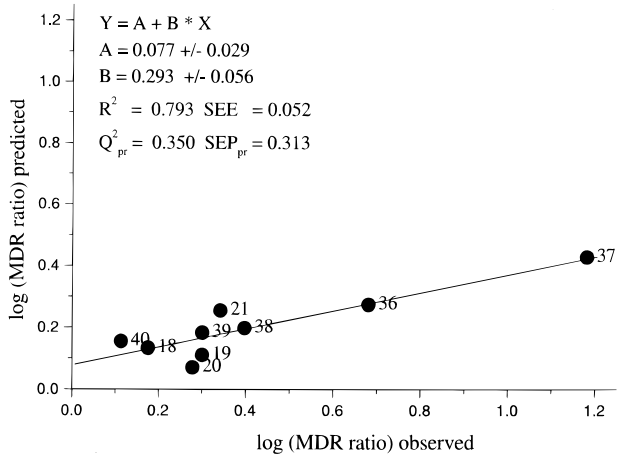

Figure 3. MDR ratios of the test compounds predicted by model BH with three components (Table 3) versus observed values; the numbered points correspond to the numbers of the compounds as assigned in Table 1.

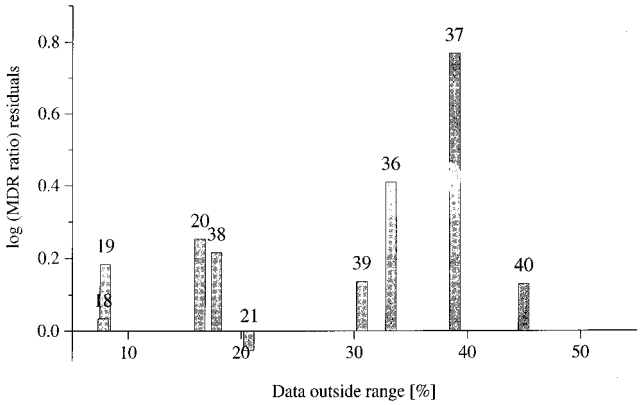

Figure 4. Data outside range (novelty) of the compounds in the test set versus residuals of the MDR ratios predicted by model BH (Table 3).

extent in relation to the drugs used for training. *trans*- and *cis*-flupentixol, 2-chlorimipramine, and quinacrine (numbers36, 37, 39, 40) were of the highest novelty (data out of range above 30%), and the thioxanthenes possessed the largest residuals as well. These results show that, in addition to the commonly recognized structural features of the MDR modulators, new structural motifs have to be included in the training set in order to improve the predictivity of the models.

Q²-GRS CoMFA Models of Phenothiazines. The results of application of Q²-GRS routine to the phenothiazine probe training set are also presented in Table 3 (B-Q²-GRS model). Comparing Q^2_{cv} of the model to the standard CoMFA B model, only a slight increase in Q^2_{cv} and decrease in SEP_{cv} was observed indicating good reproducibility of the reported models. The master region file created by the routine shows that only the peripheral boxes are missing (Figure 5). Considering the selected subregions to contain information of importance for the differences in activity, one can speculate on a possible involvement of the whole structures of the investigated drugs in interactions related to MDR reversal.

The test results of the B-Q²-GRS model were slightly lower than those of the standard CoMFA B model, and the novelty of the tested compounds changed also (Figure 6). As about one-third of the boxes were deleted

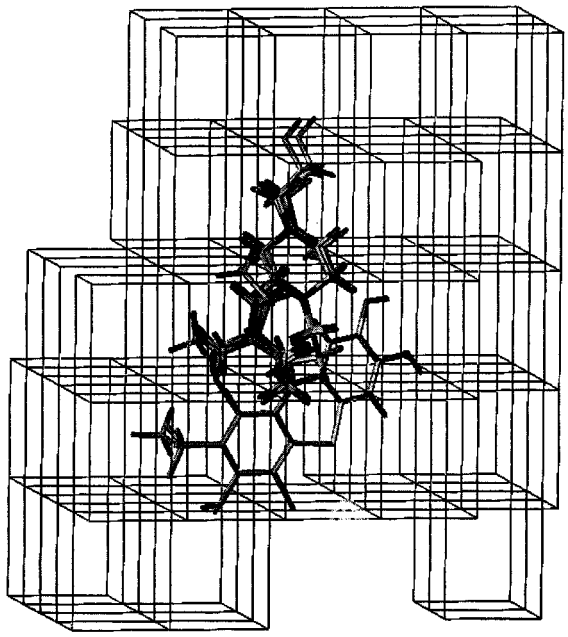

Figure 5. Master region file of B-Q²-GRS model (Table 3) showing the overlaid structures of the training compounds and the selected 82 of 125 subregions.

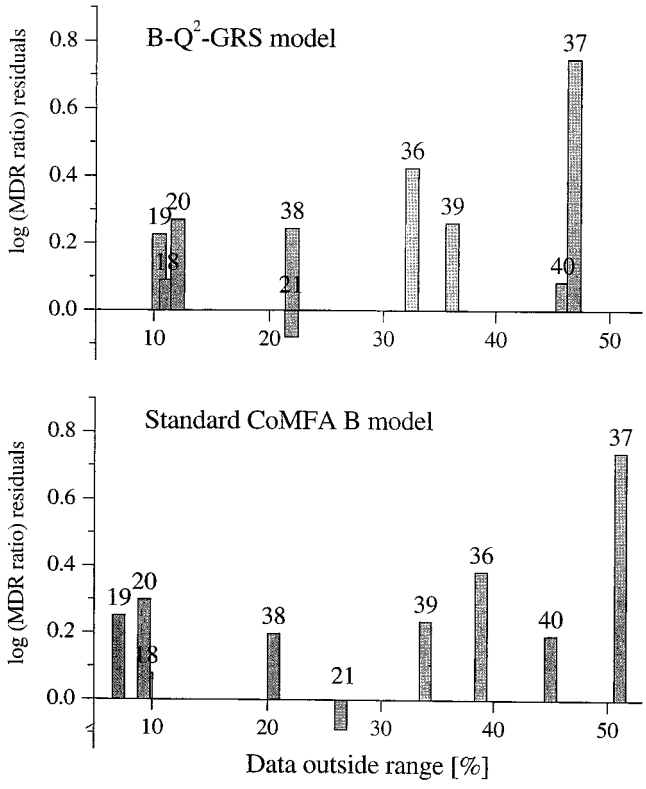

Figure 6. Data outside range (novelty) of the compounds in the test set versus residuals of the MDR ratios predicted by models B and B-Q²-GRS (Table 3).

as a result of the routine (43 of 125 subregions, Figure 6), points related to the test structures were also deleted, influencing in this way their novelty (the novelty is expressed as percent of the data of the tested drug outside the range of the training set drugs). The residuals of some drugs with the highest novelty increased (number 36−39, Figure 6), suggesting that lattice points contributing to the correct prediction of

Table 4. CoMFA Models Derived from Training Sets of Phenothiazines, Thioxanthenes, and Related Drugs: Skeleton Alignment[a]

		database alignment				field fit alignment			
training set	drug form	model[b]	field	Q^2_{cv}	SEP_{cv}	model	field	Q^2_{cv}	SEP_{cv}
phenothiazines, P; numbers 1−21	neutral, n	Pn 6	S H	0.765	0.091	Pn 14	H	0.751	0.098
		8	E H	0.753	0.097	19	E H	0.776	0.089
		10	B H	0.769	0.091	21	B H	0.725	0.096
	protonated, p	Pp 4	Ho	0.726	0.115	Pp 15	Ho	0.540	0.124
		6	S H	0.639	0.117	17	S H	0.544	0.123
		10	B Ho	0.622	0.170	18	S Ho	0.551	0.122
thioxanthenes, T; numbers, 22−37	neutral, n	Tn 4	Ho	0.769	0.210	Tn 14	H	0.518	0.350
		6	S H	0.624	0.268	15	Ho	0.734	0.226
		7	S Ho	0.616	0.260	18	S Ho	0.492	0.311
	protonated, p	Tp 2	E	0.677	0.259	Tp 14	H	0.719	0.232
		4	Ho	0.702	0.238	15	Ho	0.724	0.281
		9	E Ho	0.698	0.251	19	E H	0.694	0.252
phenothiazines and thioxanthenes, PT; numbers 1−37	neutral, n	PTn 3	H	0.784	0.176	PTn 15	Ho	0.771	0.181
		4	Ho	0.845	0.154	18	S Ho	0.713	0.206
		6	S H	0.766	0.183	20	E Ho	0.702	0.207
	protonated, p	PTp 4	Ho	0.814	0.175	PTp 14	H	0.670	0.233
		6	S H	0.778	0.176	15	Ho	0.778	0.195
		10	B H	0.781	0.175	20	E Ho	0.671	0.228
phenothiazines, thioxanthenes, and related drugs, A; numbers 1−40	neutral, n	An 3	H	0.767	0.175	An 15	Ho	0.745	0.188
		4	Ho	0.816	0.158	18	S Ho	0.712	0.195
		9	E Ho	0.777	0.169	22	B Ho	0.692	0.198
	protonated, p	Ap 4	Ho	0.771	0.191	Ap 14	H	0.679	0.218
		6	S H	0.762	0.174	15	Ho	0.793	0.181
		10	B H	0.766	0.175	21	B H	0.672	0.202

[a] Only the three models with the highest Q^2_{cv} in their sets are presented. [b] The numbering of the models obtained with the different fields and their combinations is as follows: 1, S; 2, E; 3, H; 4, Ho; 5, B; 6, S H; 7, S Ho; 8, E H; 9, E Ho; 10, B H; 11, B Ho. In case of field fit alignment 11 is added.

Table 5. CoMFA Models Derived from Training Sets of Phenothiazines, Thioxanthenes and Related Drugs: Shape Alignment[a]

		RMS fitting				field fit alignment			
training set	drug form	model[a]	field	Q^2_{cv}	SEP_{cv}	model	field	Q^2_{cv}	SEP_{cv}
phenothiazines, P; numbers 1−21	neutral, n	Pn 2	E	0.675	0.116	Pn 17	S H	0.629	0.134
		8	E H	0.693	0.108	18	S Ho	0.580	0.143
		9	E Ho	0.643	0.121	21	B H	0.620	0.113
	protonated, p	Pp 6	S H	0.608	0.127	Pp 12	S	0.564	0.117
		7	S Ho	0.503	0.143	Pp 14	H	0.550	0.127
		10	B H	0.586	0.130	16	B	0.583	0.114
thioxanthenes, T; numbers 22−37	neutral, n	Tn 3	H	0.789	0.201	Tn 14	H	0.646	0.285
		6	S H	0.792	0.199	15	Ho	0.708	0.246
		7	S Ho	0.799	0.196	20	E Ho	0.603	0.287
	protonated, p	Tp 3	H	0.625	0.267	Tp 17	S H	0.614	0.261
		6	S H	0.669	0.252	19	E H	0.593	0.268
		10	B H	0.649	0.259	21	B H	0.633	0.254
phenothiazines and thioxanthenes, PT; numbers 1−37	neutral, n	PTn 1	S	0.837	0.153	PTn 14	H	0.790	0.171
		6	S H	0.845	0.147	15	Ho	0.820	0.163
		7	S Ho	0.847	0.146	20	E Ho	0.797	0.173
	protonated, p	PTp 6	S H	0.802	0.166	PTp 17	S H	0.772	0.178
		7	S Ho	0.788	0.172	21	B H	0.777	0.176
		10	B Ho	0.791	0.171	22	B Ho	0.747	0.191
phenothiazines, thioxanthenes, and related drugs, A; numbers 1−40	neutral, n	An 6	S H	0.832	0.146	An 15	Ho	0.790	0.169
		7	S Ho	0.837	0.144	17	S H	0.780	0.170
		11	B Ho	0.824	0.150	20	E Ho	0.788	0.172
	protonated, p	Ap 6	S H	0.796	0.162	Ap 14	H	0.751	0.184
		7	S Ho	0.782	0.167	17	S H	0.767	0.172
		10	B H	0.786	0.168	21	B H	0.767	0.173

[a] Only the three models with the highest q^2_{cv} in their sets are presented. [a] The numbering of the models obtained with the different fields and their combinations is as follows: 1, S; 2, E; 3, H; 4, Ho; 5, B; 6, S H; 7, S Ho; 8, E H; 9, E Ho; 10, B H; 11, B Ho. In case of field fit alignment, 11 is added.

these structures were lost as a result of the Q^2-GRS application.

CoMFA Models of Phenothiazines, Thioxanthenes, and Related Drugs. The results of the above probe set study pointed to the necessity of developing CoMFA models from a more representative training set with a larger structural variation. Therefore, we performed training on different sets including new phenothiazines, thioxanthenes, and related drugs. The three best models of each training are presented in Tables 4 and 5 for skeleton and shape alignments, respectively. (Detailed information about all models obtained is available in Tables 4 and 5 of the Supporting Information.) In the tables the following codes are used for model designations: P, phenothiazines only; T, thioxanthenes only; PT, phenothiazines and thioxanthenes together; and A, all compounds, i.e., phenothiazines, thioxanthenes, and related drugs together; n, neutral drug forms; p, protonated drug forms. The compounds used in the training sets are given by numbers as assigned in Table 1. Each molecular field (S, E, H, Ho, B) was tried alone and in combination with

other fields in a stepwise strategy and the respective cross-validated parameters of the obtained models were recorded. Table 4 represents the results of the database and field fit and Table 5 the results of the rms fitting and field fit alignment techniques.

As seen from the tables, in almost all cases the highest Q^2_{cv} models include a hydrophobic field in both modifications: hydrophobic/polar (H) and hydrophobic only (Ho). Most of the best models from skeleton alignment contain Ho field, while for shape alignment, both H and Ho alone and in combination mainly with S field yielded the highest cross-validated predictions. No definitive preference can be given to either of both hydrophobic fields. The H field gives a slightly higher Q^2_{cv} for the models derived from the protonated forms and Ho for the neutral forms of the drugs. This observation makes sense as, in the H field, hydrophobic and polar interactions are coded, the latter ones more expressed in the protonated forms. The contribution of the hydrophobic fields, whether H or Ho, when combined with the S field is between 30 and 40% in most cases. In general, the shape models showed a Q^2_{cv} higher than the skeleton ones, especially when thioxanthenes were included in the training. Being stereoisomers, thioxanthenes can have two different shapes depending on the direction of the aliphatic chain toward the second position substituent in the ring system—in the same direction as (cis forms) or opposite to (trans form) the substituent. Shape alignment suggests a similarity in the molecular shapes that answers the observation of the stereodependent manner of MDR reversal by these drugs[17] and the stereodependent manner of their interaction with membrane phospholipids.[7]

In general, the Q^2_{cv} of the neutral forms are higher than that of the protonated ones although the drugs are mostly protonated at physiological pH. An explanation of this observation might be addressed to the long range electrostatic interactions that obscure small differences in the atomic charges of the different substituents. As a result the electrostatic field becomes flattened and the local electrostatic information is lost. Another reason may be related to a possibly imperfect parametrization of the hydrophobic constants for protonated nitrogen in the HINT fields.

To decide on the best alignment rule, both techniques proposed until now—the classic fit of selected atom pairs (database alignment and rms fitting) and field fit alignment—were studied. Field fit alignment is considered to be more "relaxed" in comparison with atom pairs fit techniques. It is based on fitting the steric and/or electrostatic fields of the template and target molecules by global rotation/translation in order to minimize the differences between the fields of both molecules. If the aligned molecules are focused to share a common global shape and location in the 3D lattice, the entropic contributions to the free energy are expected to be minimized.[24] Thus, one can expect better prediction using field fit alignment. The results of the different alignment techniques are given in Tables 4 and 5, respectively. As can be seen from the tables, in general the highest Q^2_{cv} of the field fit alignment are lower than those obtained by the classic fit of selected atom pairs. However, a more detailed comparison of Q^2_{cv} and N_{opt} for the same field and drug form in the same training set shows that no general rule can be outlined: in some models the field fit alignment gives higher, in others lower, and in others similar Q^2_{cv}. In the global models (PT and A) the field fit Q^2_{cv} values are higher than in the models of the single classes and comparable to those of the classic fit models. The results demonstrate that in this particular case the field fit alignment does not improve the CoMFA models. However, the results are close to that of the other alignment techniques and show the adequacy and applicability of the used alignment rules to the investigated problem.

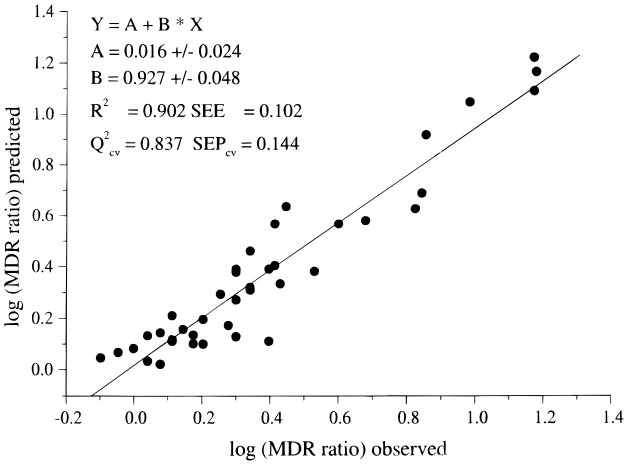

Figure 7. MDR ratios of all 40 drugs predicted by the integrated model An7 (Table 5) versus observed values.

Each chemical class individually yielded acceptable models, and their combination into one training set gave higher Q^2_{cv} values for both alignments (models PT and A in Tables 4 and 5). Figure 7 shows a plot of observed versus predicted MDR ratios for all 40 drugs used in the study by the integrated model An7 (Table 5). Cross-validated Q^2_{cv} is very close to R^2 from the non-cross-validated analysis (0.837 and 0.902, respectively), illustrating the stability of the obtained model. The improvement of the integrated model over the single class models demonstrates a better representativeness of the integrated training set for the activity investigated and indirectly confirms the suggestion of a common mechanism of MDR overcoming and common interaction sites of the drugs studied.

The best single class models were used to predict the activity of compounds from the other classes. The Q^2_{pr} values were highest for predictions of phenothiazines and related drugs from thioxanthene-derived models, partly coming close to R^2 obtained for the training sets. [The statistics of the non-cross-validated runs and the results of the test of the best single class models on the prediction of compound activities for the other classes are available as Supporting Information (Table 7).] In Figure 8 a plot of the observed MDR ratios of phenothiazines versus that predicted by the thioxanthene-trained model (Tp6, Table 5) is shown. As seen from the figure the most deviating compounds are numbers 18 and 20. These drugs possess structural fragments not included in the training set of thioxanthenes—a shorter spacer between the ring system and the basic nitrogen in the aliphatic chain (see Table 1). Removing them from the test set improves the fit significantly (R^2 = 0.752, data not shown), illustrating again the limita-

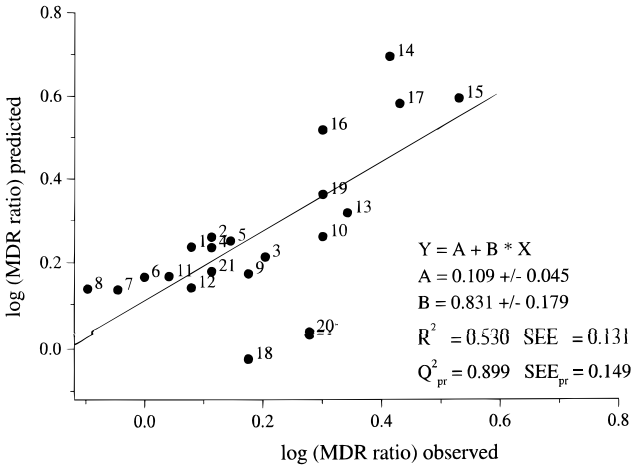

Figure 8. MDR ratios of 21 phenothiazines (numbers 1−21, Table 1) predicted by model Tp6 derived from thioxanthenes (Table 5) versus observed values.

tion of all models on predicting the influence of structural motifs not presented in the training set. According to Q^2_{pr} the thioxanthene-based models show the best prediction results in both alignments, once again shape being better (from 0.87 to 0.90) than skeleton (from 0.54 to 0.90). However no correlation between Q^2_{pr} and test R^2 can be outlined. Despite the high Q^2_{pr}, R^2 is much lower (0.40−0.68) in most cases due mainly to the large difference in the mean activity values of the training and the test set. As described in the Experimental Section, Q^2_{pr} is related to the explained variance based on the mean activity value of the training set compounds, while R^2 uses the mean activity value of the test set compounds for the evaluation of the observed variance. Thus, comparable Q^2_{pr} and R^2 are possible if the mean values of both training and test sets are also comparable. Another reason may be the greater conformational flexibility of the phenothiazine aliphatic chain and, respectively, larger uncertainty in the definition of the relevantly active conformations in this class. Indeed, shape alignment of phenothiazines gave higher Q^2_{pr} (0.36 to 0.49) than the skeleton one (0.14−0.30). As explained above, shape alignment considers the relative disposition of the ring system and N-substituted moiety in the aliphatic chain. In the thioxanthene class, for the reason of stereoisomery, the conformation flexibility of the aliphatic chain between the ring and the basic nitrogen is more limited and, correspondingly, the alignment less variable.

Figure 9 represents the graphical results of the integrated models for neutral and protonated drug forms with the superimposed structures displayed. CoMFA contour plots based on the non-cross-validated BH and BHo models for the neutral and protonated drug forms obtained by the training with all studied compounds (A coded models, Table 5) are shown. In the graphics, the colored regions correspond to the differences in the fields that are most highly associated with the differences in the investigated activity. On interpreting the graphical results, one should consider that they reflect the structural variation of the data set, on one hand, and regions of possible importance for the MDR reversal, on the other.

Sterically important regions for the neutral and protonated drugs are presented in Figure 9, parts A and B, respectively. As seen from the graphics, there are a number of small sterically forbidden regions (yellow) around the ring system which, in our opinion, can be considered as artifacts due to the alignment used, that maximize the overall shape similarity of the molecules in space. The real observations are the sterically forbidden region in proximity of the spacer between the ring system and the basic nitrogen and the favorable region (green) in the aliphatic chain distant from the basic nitrogen. In fact, the forbidden region is occupied by substances of low activity with shorter or branched spacers, and the favorable steric region in the aliphatic chain corresponds to highly active drugs with bulky substituents in this moiety.

As expected the electrostatic contours for neutral (Figure 9C) and protonated (Figure 9D) drugs show some differences. No contributing signal in the aliphatic chain can be seen for the neutral forms, whereas the protonated forms have a region of lower electron density (in blue) around the basic nitrogen. The latter suggests involvement of the protonated nitrogen in the interactions related to the activity. In both graphics, the large blue areas in the upper part of the ring system are overlapped with smaller red ones (where more electron density would increase activity), complicating in this way the interpretation of the ring substituent influence. As in the steric fields, this may result from the different orientation of the ring system and, respectively its substituents in shape alignment. However, signals related to the second position substituents were not identified in either of the drug forms, suggesting that the electrostatic properties at this position are not related to anti-MDR activity.

Parts E and F of Figure 9 represent the contour plots of hydrophobic/polar (H), and parts G and H are plots of hydrophobic only (Ho) fields. The red regions can be interpreted as areas where more hydrophobicity promotes favorable interactions, and blue ones where hydrobicity discourages them. Obviously, depending on the field and drug forms, the regions contributing to the activity are different. As seen from Figure 9G, hydrophobic/hydrophobic interactions along the whole molecular surface increase anti-MDR activity of the neutral drugs, whereas the favorable hydrophobic signal is located only in the vicinity of the ring system in the protonated forms (Figure 9H). In the case of the hydrophobic/polar interactions, a well-defined blue signal near the basic nitrogen indicates the positive influence of less lipophilic substituents on the activity of the protonated forms (Figure 9E).

The above results point to hydrophobicity as a molecular property that strongly contributes to the differences in MDR reversal effect of the drugs studied. It was postulated, based on log *P* values, that the degree of lipophilicity of phenothiazines, although important, is not the sole determinant of potency for their anti-MDR activity.[15] Our results suggest that when hydrophobicity is considered as a space directed molecular property, it can self-dependently predict anti-MDR activity of the studied drugs by a number of models and significantly improve the 3D QSAR models based on other fields. It appears that the standard CoMFA steric and electrostatic fields cannot fully describe the main forces driving the drug when reversing MDR and that

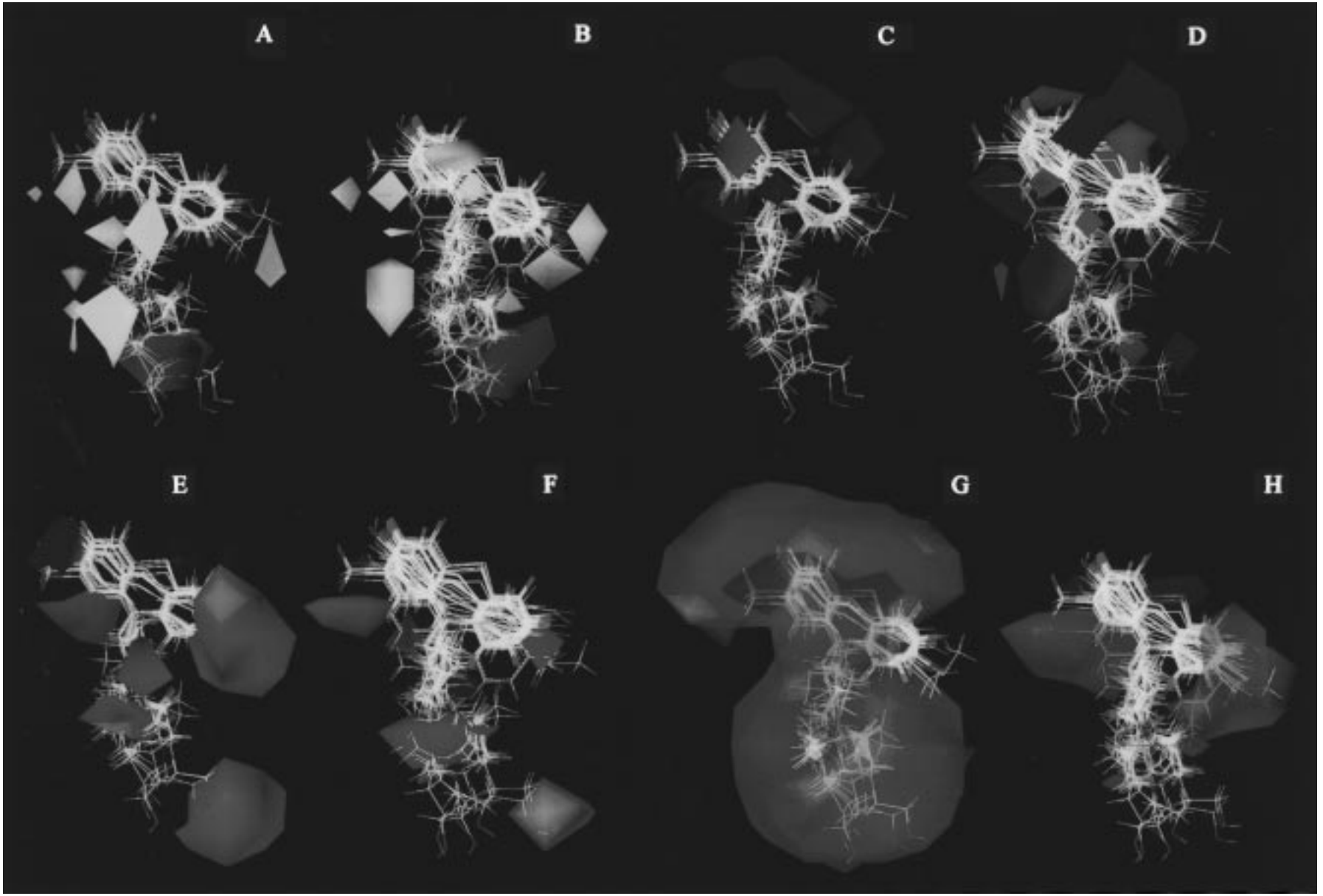

Figure 9. Graphical results with the superimposed structures displayed: (A, B) neutral and protonated steric B fields as derived from An10 and Ap10 models respectively; (C, D) neutral and protonated electrostatic B fields as derived from models An10 and Ap10, respectively; (E, F) neutral and protonated hydrophobic/polar fields as derived from models An10 and Ap10, respectively; (G, H) neutral and protonated hydrophobic only fields as derived from models An11 and Ap11, respectively. The plots are created using the "contribution*std.dev" countor mapping option, and the same percent (20 and 80) was used for all fields.

the anti-MDR effect of the studied compounds may predominantly be governed by hydrophobic forces. Indeed, when it penetrates into the membrane, the amphiphilic molecule aims to adopt a maximum hydrophobic surface, and the same might be true when interacting with hydrophobic areas at the protein binding site. The sites of action of phenothiazines and related drugs for reversal of MDR are not still identified. On the basis of the models obtained, nothing definitive can be said about the putative MDR reversal "receptor", be it a membrane phospholipid or a transport protein. As good models were obtained on the basis of data of drug conformations in a lipid environment, the results point to the involvement of drug−membrane interactions in MDR overcoming and do not reject the possibility of a direct interaction of the drugs with P-gp. Moreover, MDR-reversing compounds may be recognized by P-gp within the membrane, and consequently the transmembrane domains of P-gp may be initially involved in the interaction of the different substrates with the protein. Thus, it might prove to be that both membrane components (proteins and phospholipids) relate to MDR reversal "receptors", and to exert anti-MDR activity, the modulators have to meet the structural requirements of both the transport protein and the phospholipids surrounding it. New modeling studies are currently in progress on identification of structural features of different classes of modulators to obtain more information about MDR reversal receptor or receptors.

Conclusions

In general, there are two main questions one faces when applying CoMFA. The first question relates to the statistical predictivity of the obtained models and the second one to their interpretability in terms of the physicochemistry of the investigated drug−ligand interaction.

In the present study more than 350 CoMFA models were derived using different molecular fields and different training sets. All models obtained were statistically significant and mostly highly predictive. CoMFA parameters that could influence the 3D correlations were investigated in order to minimize the possibility of chance correlations. The neutral and monoprotonated forms were studied to get an idea about the property differences depending on charge distribution. In parallel with the standard CoMFA steric and electrostatic fields the hydrophobic fields, were also investigated in order to find the best underlying activity relationships. In fact, the best correlations were found with these fields, which shows the role of hydrophobicity for the investigated anti-MDR activity. The analysis of the graphical results from the models revealed that, in parallel with the commonly recognized critical sites (polycyclic ring system and N-substituted moiety), the molecular profile of hydrophobicity is a specific structural determinant for anti-MDR activity of the these drugs. Little research has been done on using lipophilic fields in CoMFA models, and in most cases, the interpretation of these fields is rather difficult as hydrophobicity is thought to be not really understood until now. In this particular case, however, where drug−membrane interactions are supposed to mediate the reversal of MDR, hydrophobicity is expected to play an essential role. The results confirm the suggestion of membrane-mediated mechanisms of MDR modulation. As shown above, the models based on the flupentixol geometries corresponding to those in the membrane lipid environment showed the best prediction of the test compounds. Thus, the models obtained appear to possess both statistical and physicochemical meaning, and their interpretation appears to be sensible based on realistic geometries of the investigated drugs. They can successfully be used for examining different structural moieties and their functionalities on MDR reversal to find new and more effective MDR modulators.

Experimental Section

Drugs and MDR Reversing Activity. The data used in the study are summarized from papers of Ford et al.[15,17] The sources of the compounds studied by Ford et al. are as follows: numbers 1−5, 9, 10, 14, 15, 18, 19, and 21 donated by Dr. Charles Zirkle of Smith Kline and French Laboratories (Philadelphia, PA); numbers 6, 8, 11, and 12 by Dr. Albert Manian of the National Institute of Mental Health (Bethesda, MD); number 20 by Wyeth Laboratories (Radnor, PA); number 13 by Rhone-Poulenc (Paris, France); numbers 38 and 39 by Geigy Pharmaceuticals (Summit, NJ); number 40 by Sterling-Winthrop Research Institute (Renssalear, NY); number 17 by Dr. S. J. Lucania of E. R. Squibb and Sons; the thioxanthene derivatives (numbers 22−37) by Dr. John Hyttel of H. Lundbeck (Copenhagen, Denmark); number 16 was obtained from Sigma.

MDR reversing activity in vitro in doxorubicin (DOX) resistant human breast carcinoma tumor cell line MCF-7/DOX is the biological activity of interest. MCF-7/DOX cells display a classical multidrug resistance phenotype with P-gp expression and decreased drug accumulation relative to the parental line.[15,17] The criterion used for anti-MDR activity is expressed as MDR ratio or MDR fold reversal. It is defined as IC_{50} of DOX alone, divided by IC_{50} of DOX plus the modifying drug at a drug subinhibitory concentration of $\leq IC_{10}$ and is equivalent to the increase in apparent potency of the cytotoxic agent produced by the modifier. The log values of MDR ratios were used in the CoMFA correlations as they are related to changes in linear free energy.

Computational Approaches. All molecular modeling calculations were performed on a Silicon Graphics workstation using the SYBYL 6.1/6.2 molecular modeling software.[25] The molecular modeling and 3D QSAR techniques applied were molecular mechanics (Tripos force field), quantum chemistry (MOPAC: AM1, PM3), CoMFA, HINT (Hydropathic INTeraction),[26,27] and cross-validated R^2-guided region selection (Q^2-GRS).[28] MOPAC V6 was used as implemented in SYBYL. CoMFA calculations were performed with the QSAR module of SYBYL. HINT V 2.11 and Q^2-GRS program were used as imported into the SYBYL implementation of CoMFA.

Starting Geometries and Geometry Optimization of 3D Structures. The X-ray structures of the compounds taken from the Cambridge crystallographic database[29] were used as starting conformations. Chlorpromazine (CPROMAZ refcode) and prochlorperazine (PERAZ refcode) X-ray structures were used to build, respectively, the promazine and perazine type phenothiazine derivatives for which X-ray structures were not available in the database. Local minimum conformers of *trans*- and *cis*-flupentixol obtained from the previously performed molecular modeling study[20] were used to build the respective trans and cis forms of the thioxanthene data set. Chlorimipramine and quinacrine X-ray structures were also taken from the Cambridge crystallographic database, refcodes CIMPRA and QUIANC10, respectively, and imipramine was built from chlorimipramine.

The starting structures were geometry optimized using the Tripos force field (Powell method, no electrostatics and 0.05 kcal/mol Å energy gradient convergence criterion), keeping the tricyclic ring system as an aggregate, and the final optimiza-

tion was performed with a semiempirical molecular orbital method. (According to our experience the energy minimization with the Tripos force field leads to distortions from the X-ray geometry for the tricyclic ring system, indicating that the implemented force field parameters are not suitable for this substructure.) To decide on the most suitable quantum chemical optimization technique, we performed geometry optimization (full optimization, normal convergence) of the neutral forms of chlorpromazine and perphenazine with AM1 and PM3 semiempirical methods and compared the conformations and electrostatic fields. Both methods showed very similar results (data not shown), and AM1 was finally chosen as relevant for geometry optimization and charge calculations of nitrogen containing structures.

The structures of the thioxanthenes were built from the selected conformations of *trans*- and *cis*-flupentixol as defined by an excellent agreement between NMR analysis and molecular modeling results described in detail elsewhere.[20]

As the tertiary nitrogen in the aliphatic chain of the catamphiphiles studied is mostly protonated at physiological pH, their monoprotonated structures were also generated. All sets of compounds (neutral and monoprotonated forms) were finally optimized with the AM1 Hamiltonian setting "Precise" convergence criterion.

Alignment of Molecules. The database alignment was used for skeleton, and superimposing was used for shape alignment. Trifluoperazine served as a template molecule for the training set of phenothiazines and *trans*-flupentixol for the remaining training sets.

CoMFA Specifications. CoMFA calculations were performed with the following characteristics: 2 Å grid spacing; 4 Å extension of the region beyond the van der Waals volumes of the molecules; sp^3 carbon probe atom with +1 charge; a distance dependent (1/*r*) dielectric constant. The following standard CoMFA fields were calculated: steric (S), electrostatic (E), and both (B). The same grid was used for all fields. In all calculations a field cutoff value of 30 kcal/mol with no electrostatic interactions at bad steric contacts (drop electrostatics within steric cutoff for each row) and σ_{min} of 0.2 kcal/mol were used.

The CoMFA QSAR equations were calculated by PLS leave-one-out cross-validation procedure. The models were estimated on the basis of the cross-validated R^2, Q^2_{cv}, the optimal number of components extracted, N_{opt}, and the standard error of prediction, SEP_{cv}. For the models with the highest Q^2_{cv}, the leave-one-out procedure was repeatedly performed decreasing the number of components and following the change in SEP_{cv}. The model with the minimum SEP_{cv} was compared to that with the optimal number of components, and the decrease in Q^2_{cv} was calculated. Thus, models with the optimal number of components extracted and number of components corresponding to the minimum SEP_{cv} were used further to derive the PLS non-cross-validated models characterized by the correlation coefficient, R^2, standard error of estimate, SEE, and *F* ratio.

The predictive R^2, Q^2_{pr}, was calculated for the test set compounds using the equation: $Q^2_{pr} = \sum(SD - PRESS)/SD$ with $SD = \sum(Y_{act} - Y_{mean})^2$ and $PRESS = \sum(Y_{pred} - Y_{act})^2$, where Y_{act} and Y_{pred} are the actual and predicted activities, respectively, of the compounds in the test set and Y_{mean} is the mean activity of the training set compounds.[30] The standard error of prediction, SEP_{pr}, was calculated by the equation: $SEP_{pr} = (PRESS/n)^{1/2}$, where *n* is the number of compounds in the test set. The actual versus predicted activities of the test compounds were fitted by linear regression and the explained variance R^2, SEE, and *F* ratio were recorded.

HINT Specifications. The HINT program[27] was used for the calculation of molecular lipophilic fields. Two kinds of hydrophobic fields were examined: hydrophobic/polar (H) and hydrophobic only (Ho). Both fields were calculated without cutoff. For every training set the same region as for the respective standard CoMFA fields was used.

Q^2-GRS Routine. Cross-validated R^2-guided region selection[28] divides the CoMFA region into $5 \times 5 \times 5$ (125) smaller regions and performs a CoMFA run on each of these with a grid resolution of 1 Å. To allow comparison with the conventional CoMFA procedure, σ_{min} was set to 0.2 kcal/mol. All subregions with a Q^2_{cv} larger than 0.1 were merged to form the final CoMFA region.

Acknowledgment. The authors thank the Deutsche Forschungsgemeinschaft for financial support (Grant 436 BUL 112/32/96). Parts of the work were supported also by the National Science Fund of Bulgaria (grant L-518-95) and the Fonds der Chemischen Industrie, Germany.

Supporting Information Available: Full versions of Tables 4 and 5 showing in detail the statistics for all calculated CoMFA models; Table 6 showing the detailed results of training (leave-one-out cross-validation and no validation methods) and test set predictions for different CoMFA models derived from the training on 17 skeleton aligned phenothiazines; Table 7 showing the detailed results on test set predictions by the best single class models (10 page). Ordering information is given on any current masthead page.

References

(1) Kellen, J. A. The Phenomenon of Multidrug Resistance. In *Reversal of Multidrug Resistance in Cancer*; Kellen, J. A., Ed.; CRC Press: Boca Raton, 1994; pp 1−19.
(2) Gottesman, M. M.; Pastan, I. Biochemistry of the multidrug resistance mediated by the multidrug transporter. *Annu. Rev. Biochem.* **1993**, *62*, 385−427.
(3) Ford, J. M.; Hait, W. N. Pharmacology of drugs that alter multidrug resistance in cancer. *Pharmacol. Rev.* **1990**, *42*, 156−199.
(4) Kellen, J. A. The reversal of multidrug resitance in cancer. *Anticancer Res.* **1993**, *13*, 959−961.
(5) Ford, J. Modulators of multidrug resistance. *Hematol./Oncol. Clin. North Am.* **1995**, *9*, 337−361.
(6) Gottesman, M. M. How cancer cells evade chemotherapy: sixteenth Richard and Hinda Rosenthal Foundation award lecture. *Cancer Res.* **1993**, *53*, 747−754.
(7) Pajeva, I. K.; Wiese, M.; Cordes, H.-P.; Seydel, J. K. Membrane interactions of some catamphiphilic drugs and relation to their multidrug-resistance ability. *J. Cancer Res. Clin. Oncol.* **1996**, *122*, 27−40.
(8) Wadkins, R. M.; Houghton, P. J. The role of the lipid interactions in the biological activity of modulators and multi-drug resistance. *Biochim. Biophys. Acta* **1993**, *1153*, 225−236.
(9) Liu, Q.; Hirono, S.; Moriguchi, I. Quantitative structure−activity relationships for calmodulin inhibitors. *Chem. Pharm. Bull.* **1990**, *38*, 2184−2189.
(10) Sylte, I.; Dahl, S. G. Molecular structure and dynamics of cis (Z)- and trans(E)-flupentixol and clopenthixol. *Pharm. Res.* **1990**, *8*, 462−470.
(11) Dahl, S. G.; Edvardsen, O.; Sylte, I. Molecular modelling of antipsychotic drugs and G proteincoupled receptors. *Therapie* **1991**, *46*, 453−459.
(12) Dahl, S. G.; Kollman, P. A.; Rao, S. N.; Singh, U. C. Structural changes by sulfoxidation of phenothiazine drugs. *J. Comput.-Aided Mol. Des.* **1992**, *6*, 207−222.
(13) Froimowitz, M.; Cody, V. Biologically active conformers of phenothiazines and thioxanthenes. Further evidence for a ligand model of dopamine D2 receptor antagonists. *J. Med. Chem.* **1993**, *36*, 2219−2227.
(14) Horwitz, J. P.; Massova, I.; Wiese, T. E.; Besler, B. H.; Corbett, T. H. Comparative molecular field analysis of the antitumor activity of 9H-thioxanthen-9-one derivatives against pancreatic ductal carcinoma 03. *J. Med. Chem.* **1994**, *37*, 781−786.
(15) Ford, J. M.; Prozialeck, W. C.; Hait, W. N. Structural features determining activity of phenothiazine and related drugs for inhibition of cell growth and reversal of multidrug resistance. *Mol. Pharmacol.* **1989**, *35*, 105−115.
(16) Pearce, H. L.; Winter, M. A.; Beck, W. T. Structural characteristics of compounds that modulate P-glycoprotein-associated multidrug resistance. *Adv. Enzyme Reg.* **1990**, *30*, 357−373.
(17) Ford, J. M.; Bruggeman, E. P.; Pastan, I.; Gottesmann, M.; Hait, W. N. Cellular and biochemical characterization of thioxanthenes for reversal of multidrug resistance in human and murine cell lines. *Cancer Res.* **1990**, *50*, 1748−1756.
(18) Ramu, A. Structure−activity relationship of compounds that restore sensitivity to doxorubicin in drug-resistant P388 cells. In *Resistance to Antineoplastic Drugs*; Kessel, D., Ed.; CRC Press: Boca Raton, 1989; pp 63−80.
(19) Ramu, A.; Ramu, N. Reversal of multidrug resistance by phenothiazines and structurally related compounds. *Cancer Chemother. Pharmacol.* **1992**, *30*, 165−173.

(20) Pajeva, I. K.; Wiese, M. QSAR and molecular modeling of catamphiphilic drugs able to modulate multidrug resistance in tumors. *Quant. Struct.-Act. Relat.* **1997**, *16*, 1−10.
(21) Wiese, M.; Pajeva, I. K. Molecular modeling study of the multidrug resistance modifiers cis- and trans-flupentixol. *Pharmazie* **1997**, *52*, 679−685.
(22) Kellog, G. E.; Joshi, G. S., Abracham, D. J. New tools for modelling and understanding hydrophobicity and hydrophobic interactions. *Med. Chem. Res.* **1992**, *1*, 444−453.
(23) Friche, E.; Beck, W. Molecular pharmacology of reversal of multidrug resistance and its clinical implication. In *Multidrug Resistance in Cancer Cells*; Gupta, S., Tsuruo, T., Eds.; Wiley: New York, 1996; pp 361−374.
(24) Folkers, G.; Merz, A.; Rognan, D. CoMFA: Scope and limitations. In *3D QSAR in drug design*; Kubinyi, H., Ed.; Escom: Leiden, 1993; pp 583−618.
(25) Tripos Inc., 1699 Hanley Road, St. Louis, MO 63144.
(26) Kellog, G. E.; Semus, S. F.; Abraham, D. J. HINT: A new method for empirical hydrophobic field calculation for CoMFA. *J. Comput.-Aided Mol. Des.* **1991**, *5*, 545−552.
(27) Edusoft, LC, P.O. Box 1811, Ashland, VA 23005.
(28) Cho, J. S.; Tropsha, A. Cross-validated R^2-guided region selection for comparative molecular field analysis: a simple method to achieve consistent results. *J. Med. Chem.* **1995**, *38*, 1060−1066.
(29) Cambridge Crystallographic Data Centre, University Chemical Laboratory, Lensfield Road, Cambridge CB2 1EW, U.K.
(30) Marshall, G. R. Binding-site modeling of unknown receptors. In *3D QSAR in drug design*; Kubinyi, H., Ed.; Escom: Leiden, 1993; p 109.

JM970786K